

Boosting the photoreduction activity of Cr(VI) in metal-organic frameworks by photosensitiser incorporation and framework ionization

He-Qi Zheng,^{a, 1} Xing-Hao He,^{a, 1} Yong-Nian Zeng,^a Wei-Hua Qiu,^a Jin Chen,^a Gao-Juan Cao,^a Rong-Guang Lin,^a Zu-Jin Lin,^{*a,b,c} and Banglin Chen^{*b}

^a*Department of Applied Chemistry, College of Life Science, Fujian Agriculture and Forestry University, Fuzhou, Fujian 350002, People's Republic of China. *E-mail: linzujin@fafu.edu.cn.*

^b*Department of Chemistry, University of Texas at San Antonio, One UTSA Circle, San Antonio, TX 78249-0698, United States. *E-mail: banglin.chen@utsa.edu*

^c*State Key Laboratory of Structural Chemistry, Fujian Institute of Research on the Structure of Matter, Chinese Academy of Sciences, Fuzhou, 350002, People's Republic of China.*

¹*These authors contributed equally.*

*Author to whom correspondence can be addressed: linzujin@fafu.edu.cn or banglin.chen@utsa.edu.

1- Materials and Methods

1.1 Synthesis of [bis(2,2'-bipyridine,N₁,N₁)(5,5'-dicarboxy-2,2'-bipyridine-)ruthenium(II)] - dichloride [Ru(bpy)₂(dcbpy)]Cl₂.

[Ru(bpy)₂(dcbpy)]Cl₂ was synthesized according to the published article.¹ Briefly, [Ru(bpy)₂Cl₂] (160 mg, 0.33 mmol), (2,2'-bipyridine)-5,5'-dicarboxylic acid (101 mg, 0.42 mmol), EtOH (10 mL), and H₂O (10 mL) were mixed and refluxed under N₂ atmosphere for 12 h. After cooling, the mixture was concentrated and the solid was recrystallized in MeOH/diethyl ether mixture.

1.2 Adsorption experiments

The Cr(VI) adsorption data over various MOFs was fitted by the pseudo-second-order equation, which is expressed as:

$$\frac{t}{q_t} = \frac{1}{k_2 q_e^2} + \frac{t}{q_e} \quad (1)$$

where t (min) is adsorption time; q_t (mg/g) and q_e (mg/g) are the amount of the adsorbed Cr(VI) species at time t (min) and at equilibrium, respectively; k_2 (g/(mg min)) represents the pseudo-second-order adsorption rate constant and can be calculated from the slope and intercept of plot t/q_t versus t .

Based on the pseudo second-order kinetic model, the initial adsorption rate h (mg/(g min)) and half-adsorption time $t_{1/2}$ (min) were calculated according to the following equations:

$$h = k_2 Q_e^2 \quad (2)$$

$$t_{1/2} = \frac{1}{Q_e k_2} \quad (3)$$

1.3 Photocatalytic reduction experiments

The pseudo-first-order kinetics of Langmuir-Hinshelwood was used to evaluate the reaction kinetics of Cr(VI) reduction, which is expressed as following.

$$-\ln\left(\frac{C_t}{C_0}\right) = k_1 t \quad (3)$$

where C_0 and C_t (mg g^{-1}) are the adsorption capacity of Cr(VI) at 0 and time t , respectively, and k_1 (min^{-1}) is the rate constant of the pseudo first-order model. C_0 and C_t are the concentration of Cr(VI) in reaction solution at initial time t_0 and t , respectively, and k_1 is the apparent first-order rate constant.

2- Characterization

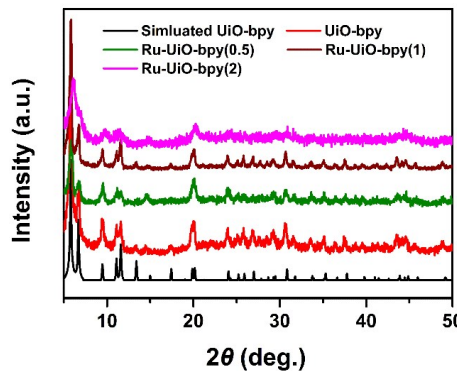


Figure S1. PXRD patterns of UiO-bpy, Ru-UiO-bpy(0.5), Ru-UiO-bpy(1), and Ru-UiO-bpy(2), respectively.

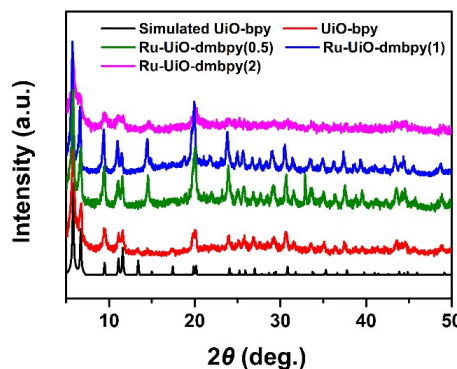


Figure S2. PXRD patterns of UiO-bpy, Ru-UiO-dmbpy(0.5), Ru-UiO-dmbpy(1), and Ru-UiO-dmbpy(2), respectively.

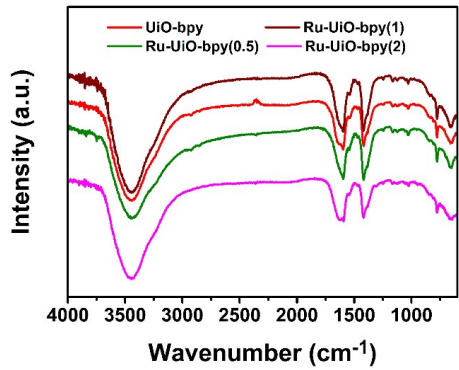


Figure S3. FT-IR spectra of UiO-bpy, Ru-UiO-bpy(0.5), Ru-UiO-bpy(1), and Ru-UiO-bpy(2), respectively.

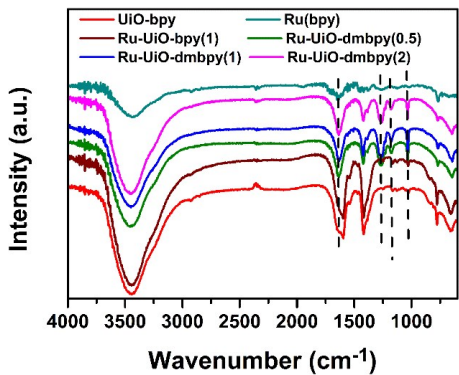


Figure S4. FT-IR spectra of UiO-bpy, Ru(bpy), Ru-UiO-bpy(1), Ru-UiO-dmbpy(0.5), Ru-UiO-dmbpy(1), and Ru-UiO-dmbpy(2), respectively.

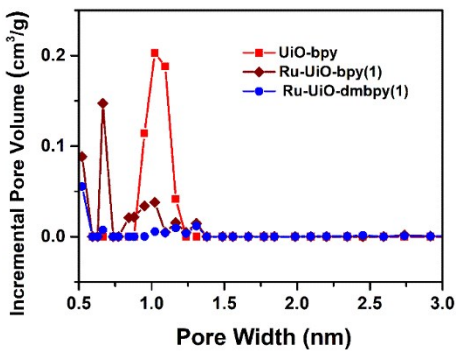


Figure S5. Pore size distributions of UiO-bpy, Ru-UiO-bpy(1), and Ru-UiO-dmbpy(1), derived from N₂ sorption isotherms based on the DFT model.

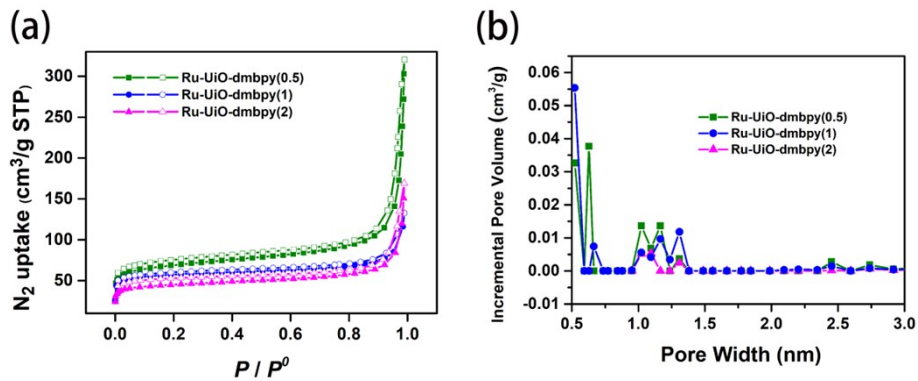


Figure S6. (a) N_2 sorption isotherms and (b) Pore size distributions of Ru-UiO-dmbpy(0.5), Ru-UiO-dmbpy(1), and Ru-UiO-dmbpy(2), respectively.

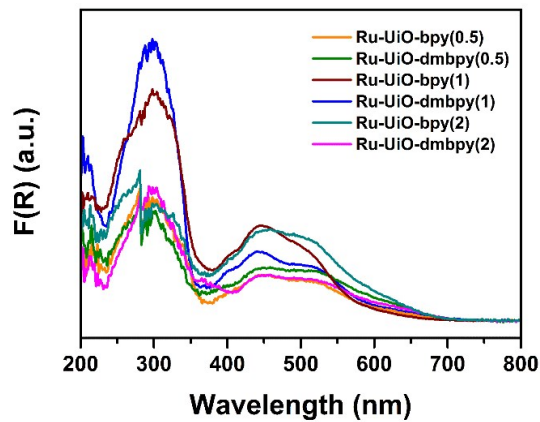


Figure S7. Solid state UV-visible diffuse reflectance spectra of Ru-UiO-bpy(0.5), Ru-UiO-dmbpy(0.5), Ru-UiO-bpy(1), Ru-UiO-dmbpy(1), Ru-UiO-bpy(2), and Ru-UiO-dmbpy(2), respectively.

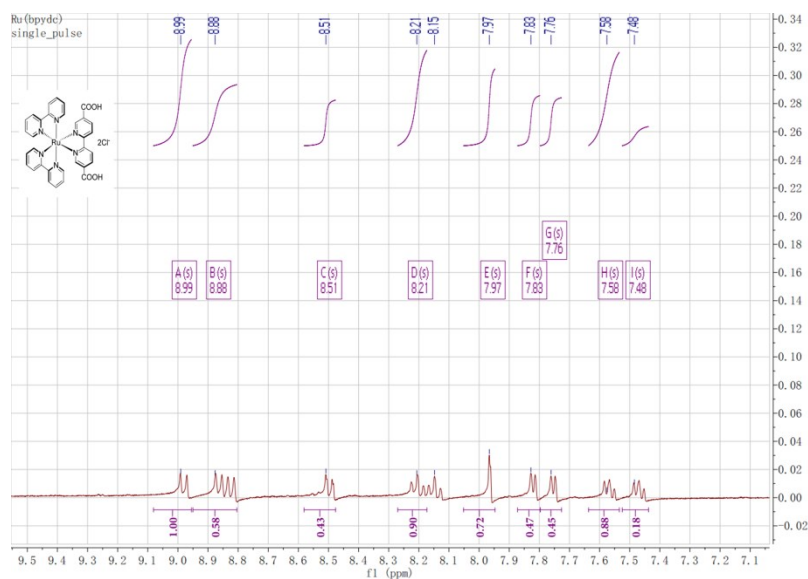


Figure S8. ^1H NMR spectrum of $[\text{Ru}(\text{bpy})_2(\text{dcbpy})]\text{Cl}_2$.

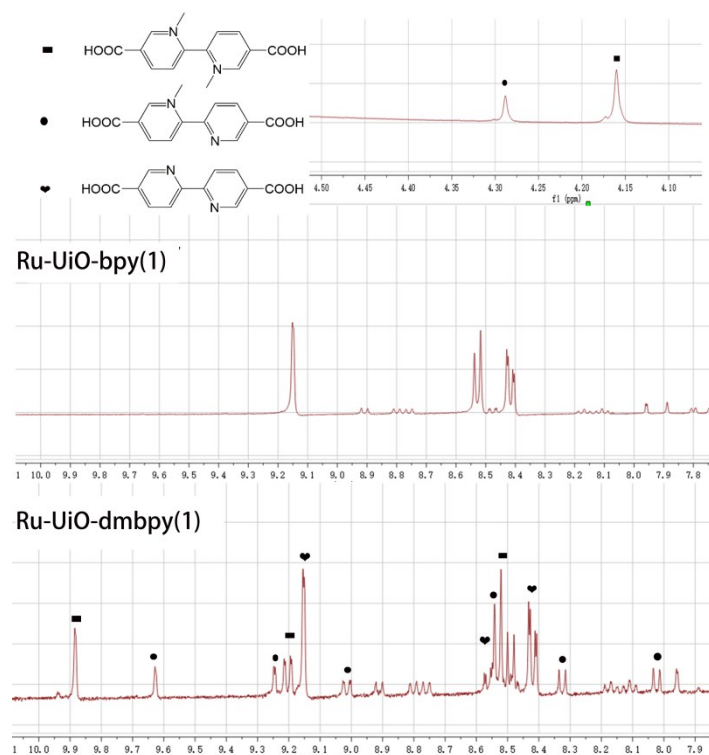


Figure S9. ^1H NMR spectra of HF-digested Ru-UiO-bpy(1) and Ru-UiO-dmbpy(1).

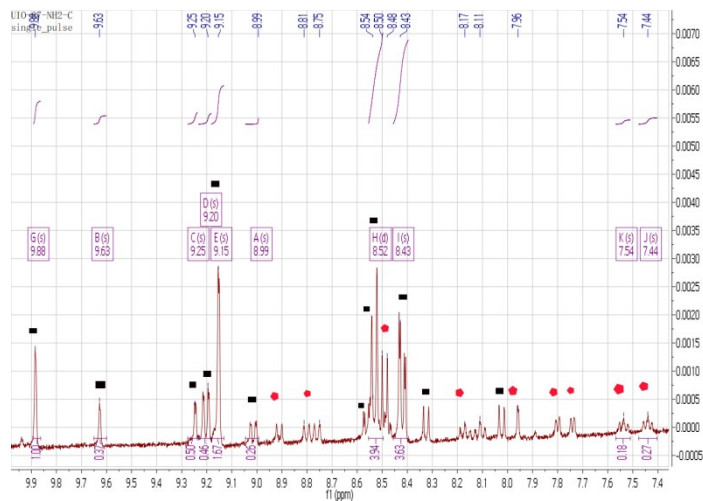


Figure S10. ^1H NMR spectrum of HF-digested Ru-Uio-dmbpy(1) in d_6 -DMSO. Red pentagons and black tetragons correspond to the signals of H₂bpydc and [Ru(bpy)₂(dcbpy)]Cl₂, respectively.

Table S1. ICP results of Ru-Uio-dmbpy.

Samples	Zr (wt%)	Ru (wt%)	Cr (wt%)	$n_{\text{Ru}}/n_{\text{Zr}}$	$n_{\text{Zr}}/n_{\text{Ru}}$
Ru-Uio-dmbpy(0.5)	13.98	0.85	-	0.0548	17.9
Ru-Uio-dmbpy(1)	14.86	0.92	-	0.0558	18.2
Ru-Uio-dmbpy(2)	13.38	1.40	-	0.0943	10.6
Recycled Ru-Uio-dmbpy(1)	15.26	0.927	0.0458	0.0942	21.8

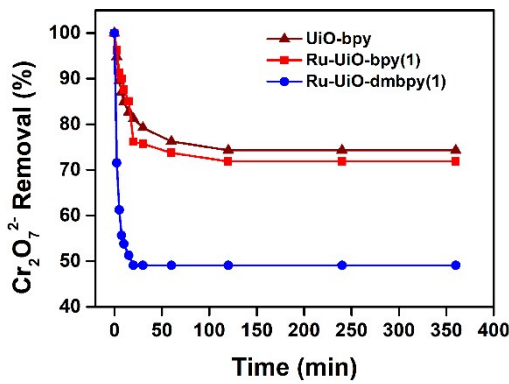


Figure S11. Effect of the contact time on the Cr₂O₇²⁻ removal over UiO-bpy, Ru-UiO-bpy(1), and Ru-UiO-dmbpy(1).

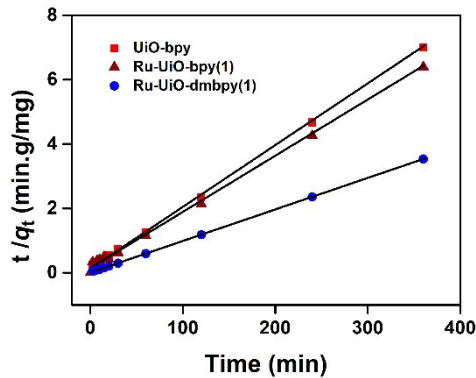


Figure S12. The pseudo-second-order kinetic fitting results of the Cr₂O₇²⁻ adsorption over UiO-bpy, Ru-UiO-bpy(1), and Ru-UiO-dmbpy(1), respectively.

Table S2. The pseudo-second-order kinetic fitting results of the Cr₂O₇²⁻ adsorption over UiO-bpy, Ru-UiO-bpy(1), and Ru-UiO-dmbpy(1).

Sample	(k ₂ , g/mg min)	(q _e , mg/g)	R ²	h (mg/g min)	t _{1/2} (min)
UiO-bpy	2.87×10 ⁻³	52.1	0.9999	7.79	6.68
Ru-UiO-bpy(1)	2.12×10 ⁻³	57.2	0.9994	6.93	8.24
Ru-UiO-dmbpy(1)	13.3×10 ⁻³	102.0	0.9999	138.4	0.74

Table S3. Comparison of the catalytic performance of Ru(bpy), UiO-bpy, Ru-UiO-bpy(1), and Ru-UiO-dmbpy(1).

Entry	Photocatalysts	scavenger	pH	Cr(VI) Reduction (%)	Rate constant (k_1 , min ⁻¹)	R ²
1	Ru(bpy)	-	3	30	0.002	0.946
2	UiO-bpy	-	3	29	0.003	0.953
3	Ru-UiO-bpy(1)	-	3	55	0.007	0.970
4	Ru-UiO-dmbpy(1)	-	3	84	0.011	0.965

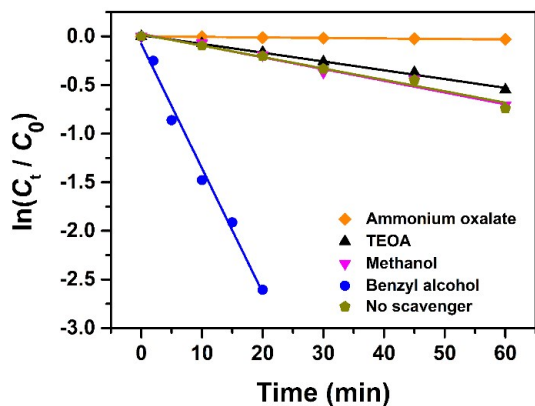


Figure S13. Plots of $\ln(C_t/C_0)$ versus reaction time for Cr(VI) reduction over various hole scavengers.

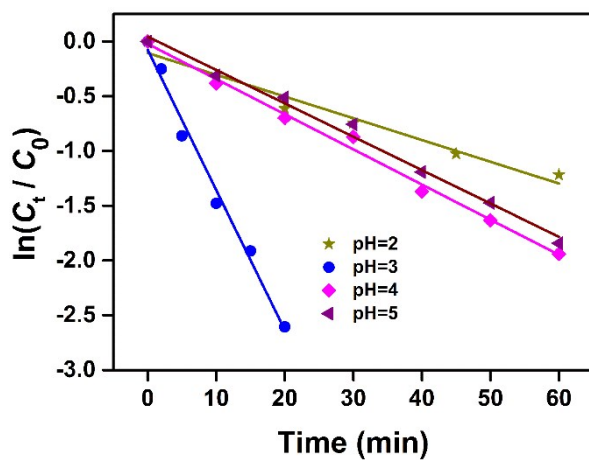


Figure S14. Plots of $\ln(C_t/C_0)$ versus time for Cr(VI) reduction over various pH.

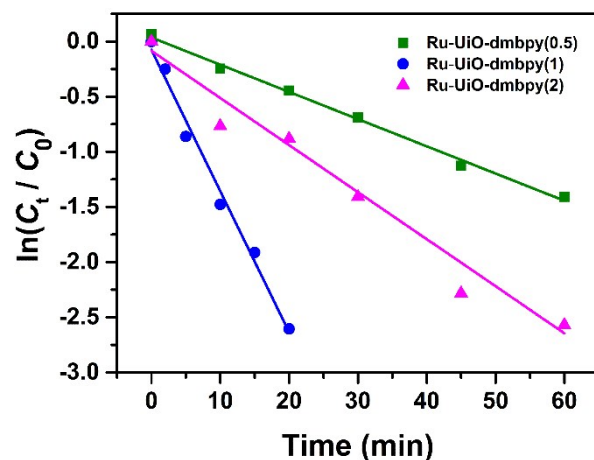


Figure S15. Plots of $\ln(C_t/C_0)$ versus time for Cr(VI) reduction over Ru-Uio-dmbpy.

Table S4. Comparison of the catalytic performance of Ru-Uio-dmbpy.

Entry	Photocatalysts	Scavenger	pH	Cr(VI) removal (%)	Rate constant (k_1 , min ⁻¹)	R^2
1	Ru-Uio-dmbpy(1)	BA	3	100	0.128	0.986
2	Ru-Uio-dmbpy(0.5)	BA	3	100	0.025	0.994
3	Ru-Uio-dmbpy(2)	BA	3	100	0.043	0.933

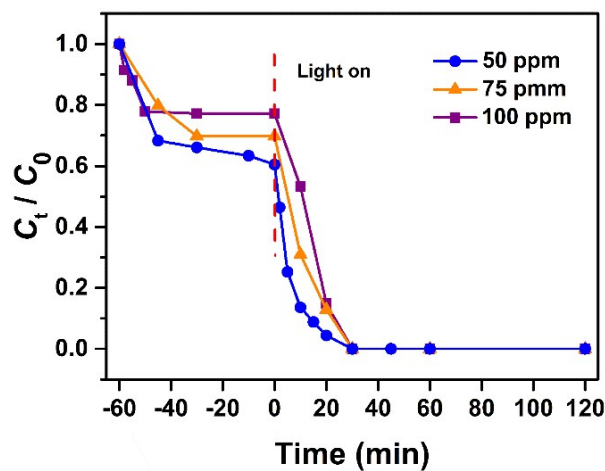


Figure S16. Effect of the initial concentration of $\text{Cr}_2\text{O}_7^{2-}$ on the photocatalytic process.

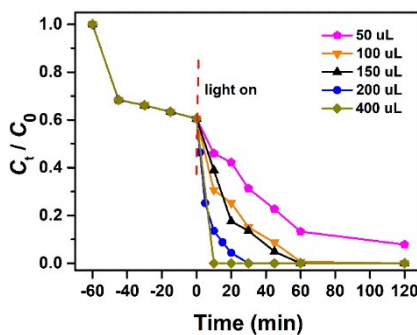


Figure S17. Effect of benzyl alcohol amount (as sacrificial agent) on the photocatalytic reduction process.

Table S5. The effect of BA amount on the photoreduction preformance of Cr(VI) over Ru-Uio-dmbpy(1).^a

Entry	Cr ₂ O ₇ ²⁻ (ppm)	Cr ₂ O ₇ ²⁻ (mL)	BA (μL)	BA (ppm)	BA/Cr(VI) (mol/mol)	Cr(VI) Conversion (%)
1	50	40	50	1300	35	57
2	50	40	100	2600	70	75
3	50	40	150	3900	105	82
4	50	40	200	5200	140	100
5	50	40	400	10400	280	100

^a irradiation by visible light for 60 min.

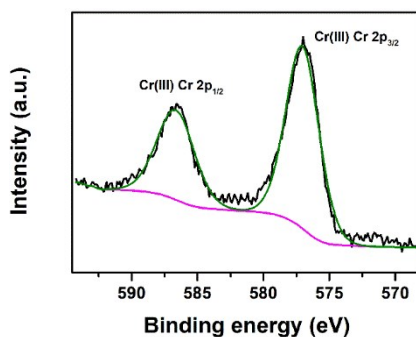


Figure S18. XPS plot of Ru-Uio-dmbpy(1) that directly collected by centrifuged after Cr(VI) reduction.

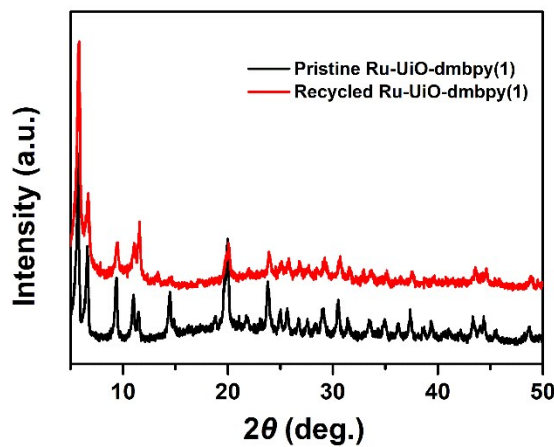


Figure S19. PXRD patterns of the pristine and recycled Ru-Uio-dmbpy(1) samples.

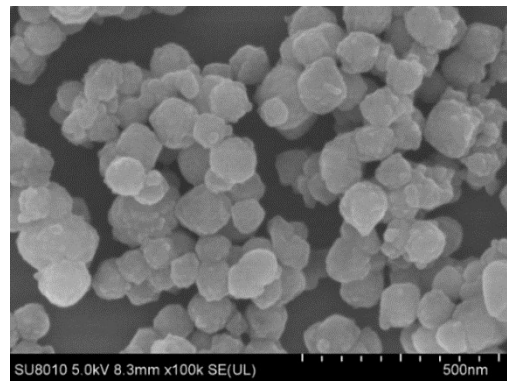


Figure S20. SEM image of recycled Ru-Uio-dmbpy(1).

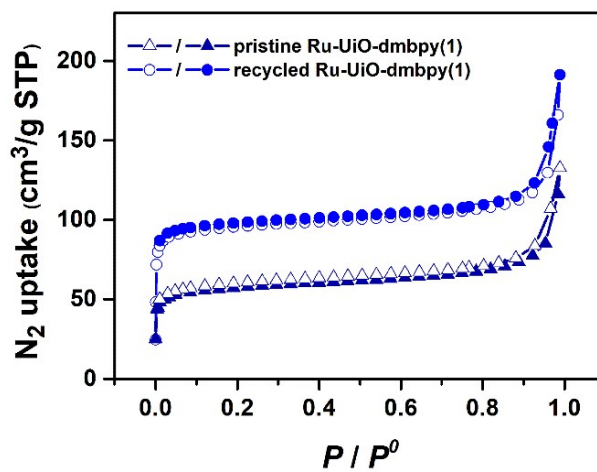


Figure S21. N_2 sorption isotherms of the pristine and recycled Ru-Uio-dmbpy(1).

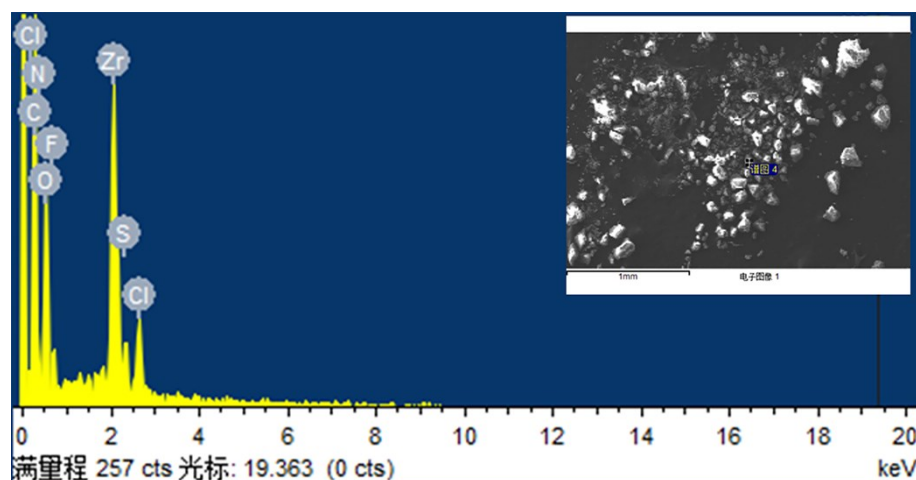


Figure S22. EDS of the recycled Ru-Uio-dmbpy(1) sample.

Table S6. The concentration of Zr and Ru in the filtrate of reaction solution after photocatalytic reaction.

Number of cycles	Zr (mg/L)	Ru (mg/L)
1	0.0146	0.126
2	0	0.185
3	0	0.137
4	0.009	0.112
5	0.0087	0.106
6	0.021	0.146
7	0.021	0.162

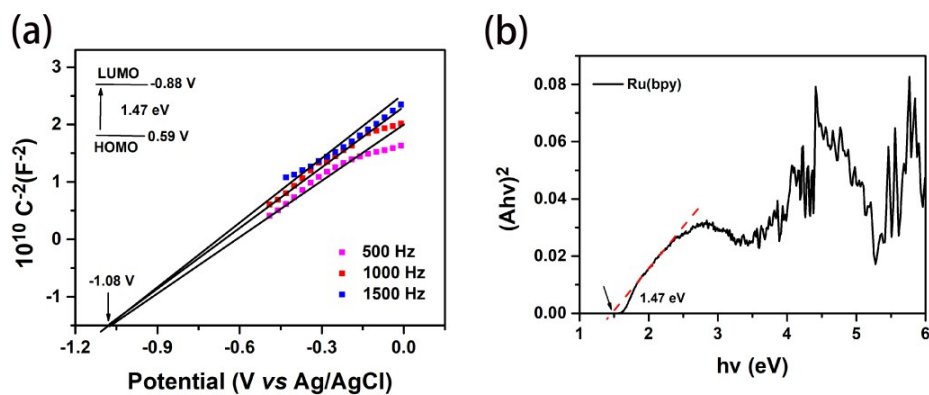


Figure S23. (a) Mott-Schottky spectra, bandgap, and (b) Tauc plot of the Ru(bpy).

Table S7. Fluorescence lifetime of Ru-UiO-bpy(1), Ru-UiO-dmbpy(1), and $\text{Cr}_2\text{O}_7^{2-}$ -@Ru-UiO-dmbpy(1) suspensions in DMF.

Sample	τ_1 (s)	Rel (%)	τ_2 (s)	Rel (%)	τ_3 (s)	Rel (%)	τ (s)
Ru-UiO-bpy(1)	4.351E-9	1.90	1.414E-7	19.95	4.682E-7	78.15	3.942E-7
Ru-UiO-dmbpy(1)	2.092E-7	15.29	6.945E-7	84.71	-	-	6.203E-7
$\text{Cr}_2\text{O}_7^{2-}$ @Ru-UiO-dmbpy(1)	1.173E-8	9.90	6.049E-8	33.28	2.930E-7	56.82	1.878E-7

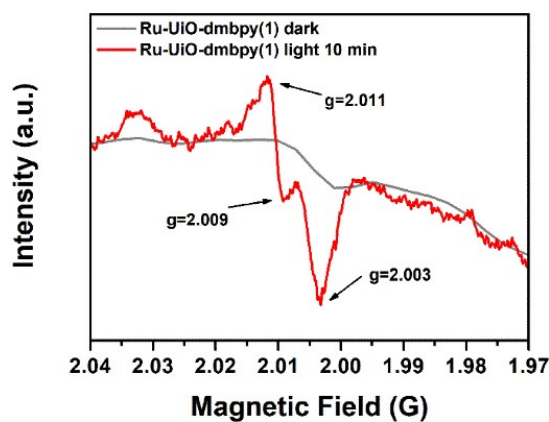


Figure S24. EPR spectra of Ru-UiO-dmbpy(1) before and after visible light irradiation for 10 min (420–780 nm).

Table S8. Comparison of the catalytic performance of Ru-U_iO-dmbpy(1) with some MOF composites and some representative inorganic photocatalysts.

Photocatalysts	Initial Cr(VI) concentration (mg/L)	Catalyst (g/L)	Irradiation time (min)	Cr(VI) reduction (%)	Rate constant (k ₁ , min ⁻¹)	Ref.
OH-TiO ₂	10	1.0	30	88	0.079	²
Bi ₂ S ₃ /C ₃ N ₄	20	1.0	60	90	0.022	³
g-C ₃ N ₄ /BiVO ₄	20	2.5	40	87	0.063	⁴
Fe-g-C ₃ N ₄ /MoS ₂	9.6	0.6	150	91.4	0.021	⁵
Ag-BiOCl	10	1.0	180	86	0.012	⁶
SrTiO ₃	4.8	1.0	240	99	0.028	⁷
BMO-S1	20	0.4	16	100	0.164	⁸
CdS-ZnIn ₂ S ₄	50	1.0	30	100	0.179	⁹
NNU-36	10	0.375	60	95.3	0.0471	¹⁰
g-C ₃ N ₄ /SnS ₂ /SnO ₂	20	0.5	60	99	0.0417	¹¹
Ag/AgCl@MIL-53(Fe)	10	0.4	240	99.4	0.0167	¹²
TiO ₂ @NH ₂ -MIL-88B(Fe)	58	0.5	35	98.6	0.0878	¹³
MIL-53(Fe)	20	1.0	40	66	0.0286	¹⁴
Fe(II)-2MI	23.8	0.1	75	100	0.021	¹⁵
MIL-68(In)-NH ₂	20	1.0	80	97	0.0368	¹⁶
H ₂ TCPP _c (I ⁻)Meim-U _i O-66	48.2	0.25	30	100	0.1541	¹⁷
g-C ₃ N ₄ /UiO-66	10	0.5	40	99	0.1102	¹⁸
JLU-MOF60	72	0.4	70	98	0.058	¹⁹
Pt@MIL-100(Fe)	20	1.0	8	100	0.5618	²⁰
Ru-U_iO-dmbpy(1)	24.1	0.25	30	100	0.128	This work

Table S9. Comparison of photocatalytic reduction of Cr(VI) over reported MOF-based catalysts.

Photocatalyst/amount (mg)	Cr(VI) solution/Volume (mL)/concentration (ppm)/pH	Sacrificial agent	Time (min)	Reduction efficiency (%)	Reduction rate (mg _{Cr(VI)} /g _{cata} / min)	Ref.
Ru-U _i O-dmbpy(1)/10	40/48.2/3.0	Benzyl alcohol (0.2 mL)	30	100	6.4	This work
Ru-U _i O-dmbpy(1)/10	40/48.2/3.0	No scavenger	30	87	5.6	This work
H ₂ TCPP \subset (I) ⁻ Meim-U _i O-66/10	40/48.2/2.0	I ⁻	30	100	6.4	¹⁷
MoO ₃ /ZIF-8/50	100/20	No scavenger	45	100	0.89	²¹
TiO ₂ @NH ₂ -MIL-88B (Fe)/20	40/58	Ammonium oxalate	35	96.8	1.1	¹³
ZCP-5/20	100/20	No scavenger	60	89	1.7	²²
g-C ₃ N ₄ /UiO-66/100	200/10/2	No scavenger	40	99	0.5	¹⁸
JLU-MOF60/10	25/72/6	No scavenger	70	98	2.6	¹⁹
UiO-66-NH ₂ (Zr/Hf)/20	40/5/2.0	No scavenger	120	98	0.08	²³
[Cu ₂ I ₂ (BPEA)][(DMF) ₄]/15	40/4.8/3.09	MeOH	10	95	1.28	²⁴
NNU-36/15	40/10/2.17	H ₂ O ₂ (1 M)	60	95.3	0.4	¹⁰
UiO-66(NH ₂)/20	40/10/2.0	Methanol (0.1 mL)	80	97	0.2	²⁵
MIL-53(Fe)/40	40/20/3.0	Ammonium oxalate (5 mg)	40	100	0.5	¹⁴

Ag/AgCl@MIL-53(Fe)/10	25/10	No scavenger	240	99.4	0.1	12
MIL-68(In)-NH ₂ /40	40/20/2.0	Ethanol (0.2 mL)	180	97	0.1	26
UiO-66(NH ₂)/20	40/10/2.0	Methanol (0.1 mL)	100	100	0.2	27
NH ₂ -MIL-88B (Fe)/20	40/8/2.0	No scavenger	50	100	0.3	28
NH ₂ -MIL-53(Fe)/20	40/8/2.0	No scavenger	60	18	0.1	28
NH ₂ -MIL-101(Fe)/20	40/8/2.0	No scavenger	60	100	0.3	28
NH ₂ -MIL-125(Ti)/20	50/48/2.1	Ethanol (2 mL)	60	97	1.9	29
NH ₂ -MIL-125(Ti)/20	50/48/2.1	No scavenger	60	80	1.6	29
MIL-125(Ti)/20	50/48/2.1	No scavenger	60	30	0.6	29
NNU-37/25	40/10/2.09	AgNO ₃ (1 mmol)	110	91.8	0.13	30
MIL-101(Cr)@NH ₂ -MIL-125(Ti)/50	50/10/2.1	No scavenger	120	72	0.1	31
Pd@UiO-66(NH ₂)/20	40/10/2.0	No scavenger	100	100	0.2	32
UiO-66(NH ₂)/20	40/10/2.0	No scavenger	100	40	0.2	32
RGO-UiO-66(NH ₂)/20	40/10/2.0	No scavenger	100	100	0.2	33
HPMo@MIL-100(Fe)/20	40/20/4.0	Ammonium oxalate (5 mg)	8	100	5.0	34
MIL-100(Fe)/20	40/20/4.0	Ammonium oxalate (5 mg)	20	80	1.6	34
MIL-100(Fe)/40	40/20/4.0	Ammonium oxalate (5 mg)	24	100	0.8	20
Au@MIL-100(Fe)/40	40/20/4.0	Ammonium oxalate (5 mg)	20	100	1.0	20

Pd@MIL-100(Fe)/40	40/20/4.0	Ammonium oxalate (5 mg)	16	100	1.3	20
Pt@MIL-100(Fe)/40	40/20/4.0	Ammonium oxalate (5 mg)	8	100	2.5	20
MIL-53(Fe)-RGO/40	40/20/4.0	Ammonium oxalate (5 mg)	80	100	0.3	35
MIL-53(Fe)/40	40/20/4.0	Ammonium oxalate (5 mg)	80	80	0.2	35

Reference

1. C. Wang, Z. Xie, K. E. deKrafft and W. Lin, *J. Am. Chem. Soc.*, 2011, **133**, 13445-13454.
2. Y. Li, Y. Bian, H. Qin, Y. Zhang and Z. Bian, *Appl. catal. B: environ.*, 2017, **206**, 293-299.
3. D. Chen, J. Fang, S. Lu, G. Zhou, W. Feng, F. Yang, Y. Chen and Z. Fang, *Appl. Surf. Sci.*, 2017, **426**, 427-436.
4. P. Babu, S. Mohanty, B. Naik and K. Parida, *Inorg. Chem.*, 2019, **58**, 12480-12491.
5. X. Wang, M. Hong, F. Zhang, Z. Zhuang and Y. Yu, *ACS Sustain. Chem. Eng.*, 2016, **4**, 4055-4063.
6. H. Li and L. Zhang, *Nanoscale*, 2014, **6**, 7805-7810.
7. D. Yang, Y. Sun, Z. Tong, Y. Nan and Z. Jiang, *J. Hazard. Mater.*, 2016, **312**, 45-54.
8. X.-Q. Qiao, Z.-W. Zhang, Q.-H. Li, D. Hou, Q. Zhang, J. Zhang, D.-S. Li, P. Feng and X. Bu, *J. Mater. Chem. A*, 2018, **6**, 22580-22589.
9. G. Zhang, D. Chen, N. Li, Q. Xu, H. Li, J. He and J. Lu, *Appl. catal. B: environ.*, 2018, **232**, 164-174.
10. H. Zhao, Q. Xia, H. Xing, D. Chen and H. Wang, *ACS Sustain. Chem. Eng.*, 2017, **5**, 4449-4456.
11. Y. Yang, X.-A. Yang, D. Leng, S.-B. Wang and W.-B. Zhang, *Chem. Eng. J.*, 2018, **335**, 491-500.
12. Q. Liu, C. Zeng, L. Ai, Z. Hao and J. Jiang, *Appl. Catal. B: Environ.*, 2018, **224**, 38-45.
13. R. Yuan, C. Yue, J. Qiu, F. Liu and A. Li, *Appl. Catal. B: Environ.*, 2019, **251**, 229-239.
14. R. Liang, F. Jing, L. Shen, N. Qin and L. Wu, *J. Hazard. Mater.*, 2015, **287**, 364-372.
15. Q. Gao, D. Lin, Y. Fan, Q. He and Q. Wang, *Chem. Eng. J.*, 2019, **374**, 10-19.
16. R. Liang, R. Huang, X. Wang, S. Ying, G. Yan and L. Wu, *Appl. Surf. Sci.*, 2019, **464**, 396-403.
17. X.-S. Wang, C.-H. Chen, F. Ichihara, M. Oshikiri, J. Liang, L. Li, Y. Li, H. Song, S. Wang, T. Zhang, Y.-B. Huang, R. Cao and J. Ye, *Appl. Catal. B: Environ.*, 2019, **253**, 323-330.

18. X.-H. Yi, S.-Q. Ma, X.-D. Du, C. Zhao, H. Fu, P. Wang and C.-C. Wang, *Chem. Eng. J.*, 2019, 121944.
19. J. Liu, Y. Ye, X. Sun, B. Liu, G. Li, Z. Liang and Y. Liu, *J. Mater. Chem. A*, 2019.
20. R. Liang, F. Jing, L. Shen, N. Qin and L. Wu, *Nano Res.*, 2015, **8**, 3237-3249.
21. Y. Zhang and S.-J. Park, *Appl. Catal. B: Environ.*, 2019, **240**, 92-101.
22. Y. Zhang and S.-J. Park, *Chem. Eng. J.*, 2019, **369**, 353-362.
23. X.-D. Du, X.-H. Yi, P. Wang, W. Zheng, J. Deng and C.-C. Wang, *Chem. Eng. J.*, 2019, **356**, 393-399.
24. D.-M. Chen, C.-X. Sun, C.-S. Liu and M. Du, *Inorg. Chem.*, 2018, **57**, 7975-7981.
25. L. Shen, S. Liang, W. Wu, R. Liang and L. Wu, *Dalton Trans.*, 2013, **42**, 13649-13657.
26. R. Liang, L. Shen, F. Jing, W. Wu, N. Qin, R. Lin and L. Wu, *Appl. Catal. B: Environ.*, 2015, **162**, 245-251.
27. L. Shen, R. Liang, M. Luo, F. Jing and L. Wu, *PCCP*, 2015, **17**, 117-121.
28. L. Shi, T. Wang, H. Zhang, K. Chang, X. Meng, H. Liu and J. Ye, *Adv. Sci.*, 2015, **2**, 1500006.
29. H. Wang, X. Yuan, Y. Wu, G. Zeng, X. Chen, L. Leng, Z. Wu, L. Jiang and H. Li, *J. Hazard. Mater.*, 2015, **286**, 187-194.
30. Z. F. Guo, H. M. Zhao, X. Liu, X. Liang, H. X. Wei, Y. C. Mei and H. Z. Xing, *Appl. Organomet. Chem.*, 2020, **34**, 10.
31. Y. Gu, Y. n. Wu, L. Li, W. Chen, F. Li and S. Kitagawa, *Angew. Chem. Int. Ed.*, 2017, **56**, 15658-15662.
32. L. Shen, W. Wu, R. Liang, R. Lin and L. Wu, *Nanoscale*, 2013, **5**, 9374-9382.
33. L. Shen, L. Huang, S. Liang, R. Liang, N. Qin and L. Wu, *RSC Advances*, 2014, **4**, 2546-2549.
34. R. Liang, R. Chen, F. Jing, N. Qin and L. Wu, *Dalton Trans.*, 2015, **44**, 18227-18236.
35. R. Liang, L. Shen, F. Jing, N. Qin and L. Wu, *ACS Appl. Mater. Inter.*, 2015, **7**, 9507-9515.